

Larry G. Mastin · Mark S. Ghiorso

Adiabatic temperature changes of magma–gas mixtures during ascent and eruption

Received: 20 October 1999 / Accepted: 15 September 2000 / Published online: 28 February 2001
© Springer-Verlag 2001

Abstract Most quantitative studies of flow dynamics in eruptive conduits during volcanic eruptions use a simplified energy equation that ignores either temperature changes, or the thermal effects of gas exsolution. In this paper we assess the effects of those simplifications by analyzing the influence of equilibrium gas exsolution and expansion on final temperatures, velocities, and liquid viscosities of magma–gas mixtures during adiabatic decompression. For a given initial pressure (p_I), temperature (T_I) and melt composition, the final temperature (T_f) and velocity (u_{max}) will vary depending on the degree to which friction and other irreversible processes reduce mechanical energy within the conduit. The final conditions range between two thermodynamic end members: (1) constant enthalpy ($dh=0$), in which T_f is maximal and no energy goes into lifting or acceleration; and (2) constant entropy ($ds=0$), in which T_f is minimal and maximum energy goes into lifting and acceleration. For $ds=0$, $T_I=900$ °C and $p_I=200$ MPa, a water-saturated albitic melt cools by ~ 200 °C during decompression, but only about 25% of this temperature decrease can be attributed to the energy of gas exsolution per se: the remainder results from expansion of gas that has already exsolved. For the same T_I and p_I , and $dh=0$, T_f is 10–15 °C hotter than T_I but is about 10–25 °C cooler than T_f in similar calculations that ignore the energy of gas exsolution. For $ds=0$, $p_I=200$ MPa and $T_I=900$ °C, assuming that all the enthalpy change of decompression goes into kinetic energy, a water-saturated albitic mixture can theoretically accelerate to ~ 800 m/s. Similar calculations that ignore gas exsolution (but take into account gas expansion) give

velocities about 10–15% higher. For the same T_I , $p_I=200$ MPa, and $ds=0$, the cooling associated with gas expansion and exsolution increases final melt viscosity more than 2.5 orders of magnitude. For $dh=0$, isenthalpic heating decreases final melt viscosity by about 0.7 orders of magnitude. Thermal effects of gas exsolution are responsible for less than 10% of these viscosity changes. Isenthalpic heating could significantly reduce flow resistance in eruptive conduits if heat generation were concentrated along conduit walls, where shearing is greatest. Isentropic cooling could enhance clast fragmentation in near-surface vents in cases where extremely rapid pressure drops reduce gas temperatures and chill the margins of expanding pyroclasts.

Introduction

The violent processes that accompany volcanic eruptions – high ejection velocities, convective uplift, production of shock waves, etc. – result largely from the conversion of thermal energy stored in magmas to mechanical energy. Yet numerical programs designed to calculate flow properties in eruptive conduits, with only a few exceptions (Buresti and Casarosa 1989; Wohletz and Valentine 1990; Mastin 1995a, 1997), assume that temperatures within the conduit remain constant. Those that do calculate temperature changes assume that the mass fraction of gas in the erupting mixture does not change with pressure (Buresti and Casarosa 1989) or do not take the energy of gas exsolution into account in the energy budget (Wohletz and Valentine 1990; Mastin 1995a, 1997). Only two models (Proussevitch and Sahagian 1998; Mastin 2000) consider the non-isothermal flow in eruptive conduits and incorporate thermal effects of gas exsolution.

To date, the question of how the energy of gas exsolution affects eruptive processes has not been directly addressed. Several studies have estimated thermodynamic parameters that control gas exsolution (e.g.,

L.G. Mastin (✉)
US Geological Survey, Cascades Volcano Observatory,
5400 MacArthur Blvd., Vancouver, WA 98661, USA
E-mail: lgmastin@usgs.gov

M.S. Ghiorso
Department of Geological Sciences, University of Washington,
Seattle, WA 98195-1310, USA

Editorial responsibility: T.L. Grove

Burnham and Davis 1971, 1974; Nicholls 1980; Nicholls and Stout 1982; Ghiorso et al. 1983; Silver and Stolper 1985; Ghiorso and Sack 1995; Papale 1997). One study (Sahagian and Proussevitch 1996) estimates the effect of gas exsolution on the final temperatures of decompressed albite–water mixtures. None of these studies, however, considers the effect of gas exsolution on the energetics of conduit flow.

Theory

We limit our analysis to conditions under which magma–gas mixtures do not lose significant heat or gas to the surrounding wall rock during transport. These conditions are most closely met when mass-flux rates are high; specifically in Plinian, sub-Plinian, and basaltic lava-fountain eruptions. Conductive heat loss into the host rock during such eruptions is at least a few orders of magnitude less than heat flux through the conduit by mass flow (Woods 1995). Similarly, gas loss through conduit walls can be low for high flux rate eruptions (Jaupart and Allègre 1991), though in low flux rate eruptions it can dominate flow processes (Eichelberger et al. 1986).

We calculate temperature change using the following energy equation (Moran and Shapiro 1992, p. 123; see Table 1 for a list of variables):

$$h + \frac{u^2}{2} + gz = \text{constant} \quad (1)$$

The equation states simply that the sum of enthalpy plus kinetic energy plus elevation potential energy per unit mass (the first three terms on the left, respectively) is constant. Equation (1) assumes that no heat, work, or mass is transferred into or out of the mixture. It makes no assumptions regarding the reversibility of the process, or the presence or absence of phase changes or chemical reactions within the system.

If one considers that temperature is related to enthalpy, it is apparent from Eq. (1) that the final temperature of the mixture is not unique. Mixtures that accelerate and rise to great heights will have more kinetic and potential energy, and less enthalpy (be cooler) in their final state than those that do not rise or accelerate. Lifting 1 kg of magma 4 km would cool it by about 40 °C [assuming that $g\Delta z = c_{pm}\Delta T$, and c_{pm} , the specific heat, ≈ 1 kJ/(kg K)]. Accelerating it to 200 m/s would cool it about 20 °C.

Without a model that explicitly calculates acceleration and lifting in an eruptive conduit, one cannot determine the values of the terms in Eq. (1). One can, however, establish minima and maxima for them:

1. If no energy goes into acceleration or lifting, then $h = \text{constant}$ and cooling is minimal. Fluids decompress under constant-enthalpy (isenthalpic) conditions if friction (primarily viscous shearing) is so great as to recycle all kinetic energy back into heat.

Hydrothermal fluids flowing through porous media are assumed to decompress isenthalpically (e.g., Hayba and Ingebritsen 1997), as are industrial fluids driven through porous filters under high pressure gradients (Moran and Shapiro 1992, p. 498). Phreatic eruptions have been studied as isenthalpic processes (White 1955; Muffler et al. 1971), although kinetic and lifting energies may be significant in some of them. For magma–gas mixtures, decompression most closely approaches isenthalpic when ascent velocities are low and expansion is minimal – usually at great depth in an eruptive conduit.

2. If no friction or other irreversible process impedes lifting or acceleration, then cooling is maximal and the entropy of the erupting mixture is constant. The constancy of entropy under these conditions can be demonstrated by differentiating Eq. (1) and substituting dh with its thermodynamic equivalent ($dq + vdp$):

$$dq + vdp + udu + gdz = 0 \quad (2)$$

Under adiabatic conditions [assumed for Eq. (1)], changes in heat (dq) occur only as a result of irreversible processes. Primary among these is friction, which dissipates kinetic energy and recycles it into heat. Resistance to bubble expansion by a viscous melt will also convert kinetic energy into heat, as will irreversible gas exsolution (Sahagian and Proussevitch 1996).

The change in specific entropy (s) of a system is defined as $ds \equiv dq/T$. If no heat is generated, the entropy does not change and the process is reversible. Gas flow through engineered, frictionless nozzles (Moran and Shapiro 1992, p. 234) is nearly isentropic and much of gas dynamics theory is predicated on the assumption of constant entropy (e.g., Liepmann and Roshko 1957; Saad 1985). Several studies of erupting magma–gas mixtures have also assumed constant-entropy decompression (Kieffer and Delany 1979; Kieffer 1981, 1984; Wohletz 1986; Mastin 1995b). Decompression of magma–gas mixtures most closely approaches isentropic in cases where gas expansion is maximal and velocities are high, such as in a flaring eruptive vent at the Earth's surface.

Assumptions and simplifications

The objective of this study is to calculate the change in temperature of decompressing melt–gas mixtures under isentropic and isenthalpic conditions, with and without gas exsolution. To simplify our calculations, we assume that: (1) chemical changes in the erupting mixture involve only gas exsolution (i.e., crystal growth is ignored); (2) the gas phase is purely H₂O; and (3) gas and melt remain in thermal equilibrium. Violation of condition (1) will likely slightly increase final temperatures. Violation of condition (3) may produce heterogeneous temperatures but will not significantly affect the average bulk temperature. Intro-

Table 1 List of variables

Variable	Description	Units
C	Sound speed	m/s
c_p	Specific heat at constant pressure	J/(kg K)
c_v	Specific heat at constant volume	J/(kg K)
f	Fugacity	Pa
G_∞	Elastic shear modulus	Pa
g	Gravitational constant	m/s ²
h	Specific enthalpy	J/kg
\bar{h}	Molar enthalpy	J/mol
K	Empirical constant used to calculate brittle failure	dimensionless
k	Bulk modulus	Pa
m_i	Mass fraction of component i in system (melt + gas)	Dimensionless
\hat{m}_i	Mass fraction of component i in melt	Dimensionless
M_i	Mass of component i in melt	kg
M_{tot}	Total mass of melt	kg
M_{tot}	Total mass of system (melt + gas)	kg
p	Pressure	Pa or MPa
q	Heat	J/kg
R	Universal gas constant (8.314 J/mol K)	J/(mol K)
s	Specific entropy	J/(kg K)
\bar{s}	Molar entropy	J/(mol K)
T	Temperature	C or K
u	Velocity	m/s
v	Specific volume	m ³ /kg
\bar{v}	Molar volume	m ³ /mol
w_i	Molecular weight of component i	kg/mol
w_{ij}	Interaction coefficient between components i and j	J/mol
x_i	Mole fraction of component i	Dimensionless
X	Total number of moles	moles
z	Vertical position (positive upwards)	m
β	Empirical gas solubility constant	Dimensionless
Φ_p	Integral of vdp , where v is the partial molar volume of dissolved water in a melt	J/mol
ϕ	Volume fraction gas	Dimensionless
$\dot{\epsilon}$	Strain rate	s ⁻¹
η	Viscosity	Pa s
γ_w	Activity coefficient of water in melt	Dimensionless
μ	Chemical potential	J/kg
$\bar{\mu}$	Molar chemical potential	J/mol
ρ	Density	kg/m ³
σ	Empirical gas solubility constant	Pa ^{-β}
Subscripts		
f	Final state (after decompression)	
g	Gas phase	
i,j	Component i or j in melt	
m	Liquid (melt) phase	
max	Maximum (e.g., u_{max} = maximum theoretical velocity)	
p	Constant pressure	
T	Constant temperature	
tot	Total	
v	Constant volume	
w	H ₂ O (water) component	
l	Initial state (prior to decompression)	
Superscripts		
o	Standard state	

duction of a non-aqueous gas component (such as CO₂) will affect the solubility of the gas phases, the entropy and enthalpy of exsolution, and the thermal effect of gas expansion. For reasons outlined in Appendix A, we expect the enthalpy and entropy of exsolution of CO₂ to be of the same order of magnitude as for H₂O.

In order to derive equations for the change in temperature with pressure (dT/dp), we require a simple

relation between the mass fraction of dissolved water in the melt (\hat{m}_w) and pressure (p) that can be easily differentiated. We use the following:

$$\hat{m}_w = \sigma p^\beta \quad (3)$$

where σ and β are empirically determined constants. At pressures below a few hundred megapascals this equation reproduces experimental data to a reasonable level of accuracy and has been used in most conduit models

(e.g., Wilson et al. 1980; Giberti and Wilson 1990; Dobran 1992).

The mass fractions of melt (m_m) and gas (m_g) in the total system can be calculated from Eq. (3) as:

$$m_g = m_w - m_m \hat{m}_w \text{ if } m_w > m_m \sigma p^\beta \quad (4a)$$

$$m_g = 0, \text{ if } m_w \leq m_m \sigma p^\beta \quad (4b)$$

$$m_m = 1 - m_g \quad (4c)$$

where m_w is the total mass fraction of water (exsolved plus dissolved) in the system.

Methods of solution

We assume a thermodynamic system consisting of a silicate melt and water. The system may initially contain a single phase (melt), or two phases (melt plus gas) depending on whether the amount of water present exceeds that which can dissolve in the melt. The specific enthalpy, h , and entropy, s , of the mixture are sums of s and h of the two phases multiplied by their respective mass fractions:

$$h = m_g h_g + m_m h_m \quad (5)$$

$$s = m_g s_g + m_m s_m \quad (6)$$

For a given p and T , h_g and s_g can be calculated (Haar et al. 1984), as can h_m and s_m if the composition of the melt is known (Ghiorso and Sack 1995). Similarly, m_g and m_m can be determined if the total water content and its solubility in the melt are known.

Thus for a given initial pressure, temperature, and chemical composition, the value of h or s can be calculated. After decompression, the final pressure of the system is known, as well as m_g , m_m [from Eq. (4a–c)], and the composition of the melt. Thus one can simply adjust the final temperature until the final entropy or enthalpy equals the initial value. Because h and s are state functions, the thermodynamic path does not have to be known to calculate final temperature.

This method is simple and it can be performed without formulating and integrating differential equations for dT/dp . However, it has the disadvantage that one cannot see the mathematical terms that govern cooling due to expansion, decompression, and gas exsolution. Without being able to identify those terms, one cannot evaluate their importance or judge the effect of uncertainties in their numerical values. Therefore we derive the differential equations below. We check their correctness by integrating them and comparing their results with those obtained from the method above.

dT/dp for isenthalpic decompression

We derive dT/dp for isenthalpic decompression by differentiating Eq. (5):

$$dh = d(m_g h_g + m_m h_m) = m_g dh_g + m_m dh_m + h_g dm_g + h_m dm_m = 0 \quad (7)$$

We evaluate m_m , and m_g as described above, and obtain dm_g and dm_m by differentiating Eq. (4a–c) (see Appendix B) to give:

$$dm_g = -\frac{m_m \hat{m}_w \beta}{(1 - \hat{m}_w) p} dp \quad m_w > m_m \sigma p^\beta \quad (8a)$$

$$= 0 \quad m_w \leq m_m \sigma p^\beta \quad (8b)$$

$$dm_m = -\frac{m_m \hat{m}_w \beta}{(1 - \hat{m}_w) p} dp \quad m_w > m_m \sigma p^\beta \quad (9a)$$

$$m_w \leq m_m \sigma p^\beta \quad (9b)$$

We derive dh_g as follows:

$$dh_g = \left(\frac{\partial h_g}{\partial T}\right)_p dT + \left(\frac{\partial h_g}{\partial p}\right)_T dp = c_{pg} dT + \left[v_g - T \left(\frac{\partial v_g}{\partial T}\right) \right] dp \quad (10)$$

The change in enthalpy of the melt (dh_m) is the sum of the partial differentials with respect to p , T , and the mass (\hat{M}_w) of dissolved water, holding the masses of all other components, \hat{M}_j (SiO_2 , TiO_2 , etc.) constant:

$$dh_m = \left(\frac{\partial h_m}{\partial T}\right)_{p, \hat{M}_j} dT + \left(\frac{\partial h_m}{\partial p}\right)_{T, \hat{M}_j} dp + \left(\frac{\partial h_m}{\partial \hat{M}_w}\right)_{T, p, \hat{M}_j \neq \hat{M}_w} d\hat{M}_w \quad (11)$$

It is shown in Appendix C that:

$$\left(\frac{\partial h_m}{\partial \hat{M}_w}\right) d\hat{M}_w = \frac{\hat{m}_w \beta}{(1 - \hat{m}_w) p} (h_w - h_m) dp \quad (12)$$

where h_w is the partial enthalpy of dissolved water in the melt per unit mass water. Substituting Eq. (12) into Eq. (11) and making the same substitutions for the partials with respect to p and T as were used in Eq. (10), we obtain:

$$dh_m = c_{pm} dT + \left\{ \left[v_m - T \left(\frac{\partial v_m}{\partial T}\right)_p \right] + \frac{\hat{m}_w \beta}{(1 - \hat{m}_w) p} (h_w - h_m) \right\} dp \quad (13)$$

Substituting the above expressions for dh_g , dh_m , dm_g and dm_m into Eq. (7) and rearranging, we obtain the following expression for the isenthalpic change in temperature with pressure for water-saturated melts:

$$\frac{dT}{dp} = \frac{-m_m \left[v_m - T \left(\frac{\partial v_m}{\partial T}\right) \right] - m_g \left[v_g - T \left(\frac{\partial v_g}{\partial T}\right) \right] + \frac{m_m \hat{m}_w \beta}{(1 - \hat{m}_w) p} (h_g - h_w)}{m_g c_{pg} + m_m c_{pm}} \quad (14)$$

The first two terms in the numerator, $m_m [v_m - T(\partial v_m/\partial T)]$ and $m_g [v_g - T(\partial v_g/\partial T)]$, give the effect of expansion and decompression of the liquid and gas phases, respectively, on cooling. The third term gives the cooling effect of gas exsolution. Equation (14) has the following implications:

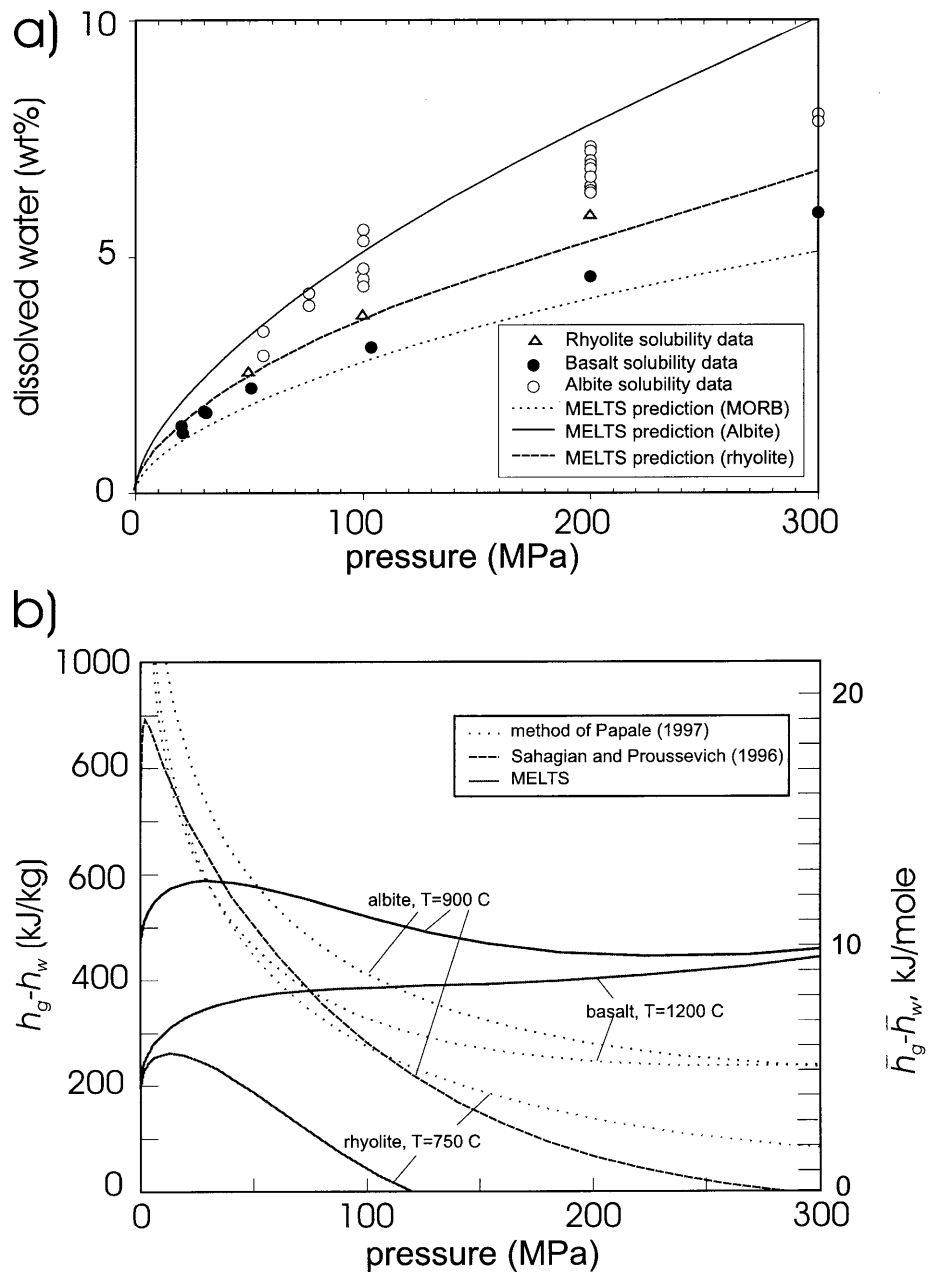
1. For a single-phase liquid with no exsolving gas and $(\partial v_m/\partial T) = 0$, $dT/dp = -v_m/c_{pm}$. The minus sign on the

$s_w = -(\partial\mu_w/\partial T)$ and $h_w = \mu_w + Ts_w$. In turn, μ_w can be constrained from experimental data based on the fact that, at saturation, μ_w equals the chemical potential of water in the gas phase (μ_g). In their program MELTS, Ghiorso and Sack (1995) use a method for calculating μ_w modified from Nicholls (1980). The method of Ghiorso and Sack (1995) predicts H₂O solubility reasonably well at pressures below a few hundred megapascals (Fig. 2a). Ghiorso and Sack calculate the chemical potential of water as follows:

$$\begin{aligned} \bar{\mu}_w = & RT \left(\frac{A}{T} + B \right) + \Phi_p + \bar{\mu}_{g,Haar}(T, 1atm) - \bar{\mu}_{g,Robie}(T, 1atm) \\ & + 2RT \ln x_w + \sum_{i=1}^n w_{wi} x_i - \frac{1}{2} \sum_{i=1}^n \sum_{j=1}^n w_{ij} x_i x_j \end{aligned} \quad (22)$$

where A and B are empirically derived constants; w_{ij} are empirically derived interaction terms between components i and j [e.g., between SiO₂ and TiO₂, using the complex oxides defined in Ghiorso and Sack (1995) as the individual components]; $\bar{\mu}_{g,Haar}$ and $\bar{\mu}_{g,Robie}$ are the molar chemical potentials of gaseous H₂O at 0.1 MPa pressure, calculated using methods of Haar et al. (1984) and Robie et al. (1978), respectively; w_{wi} (a subset of w_{ij}) are interaction coefficients between dissolved water and some component i ; x_i is the mole fraction of component i ; x_j is the mole fraction of component j ; and Φ_p is the integral of the partial molar volume of dissolved water (\bar{v}_w) with pressure, evaluated at the temperature of interest, and integrated from $p=0$ Pa to the pressure of interest:

Fig. 2 a Dissolved water versus pressure for water-saturated albite, rhyolite, and MORB basalt. Symbols represent experimental data from Hamilton and Oxtoby (1986) for albite, Dixon et al. (1995) for MORB basalt, and Holtz et al. (1995) for rhyolite. Lines give saturation values for these magma types predicted by Eq. (22). **b** Enthalpy difference ($h_g - h_w$) versus pressure for the three magma types given in a, using methods of solution from MELTS [Eq. (25)], Papale (Appendix A), and Sahagian and Proussevitch (1996)



$$\Phi_p = \int_0^p \bar{v}_w dp \quad (23)$$

The MELTS program of Ghiorso and Sack (1995) uses values of A ($-33,676.0$ J/mol K) and B (18.3527 J/mol) that are optimized for data on water solubility. The values of the interaction coefficients w were determined by Ghiorso and Sack (1995) through multivariate regression of more than 15,000 experimental data on silicate melts. The overlines above each term ($\bar{\mu}_w$, for example) indicate that they are given per mole H_2O , rather than per kilogram, in contrast to s and h in earlier equations.

We calculate \bar{v}_w using a 3-D polynomial function of p and T derived by Burnham and Davis (1974) for albite–water melts, which gives $\bar{v}_w \approx 18\text{--}34$ cm^3/mol for pressures of 0.1–200 MPa and temperatures of 700–11,000 °C. More recent studies (Ochs and Lange 1997, 1999) give values that differ somewhat from those of Burnham and Davis (1974), but those differences do not significantly affect the results of this study.

From the relation $s_w = -(\partial\bar{\mu}_w/\partial T)$, the difference $\bar{s}_g - \bar{s}_w$ can be derived from Eq. (22):

$$\begin{aligned} \bar{s}_g - \bar{s}_w = & \bar{s}_g + RB + \left(\frac{\partial\Phi_p}{\partial T}\right)_p + \bar{s}_{g,Robie}(T, 1atm) \\ & - \bar{s}_{g,Haar}(T, 1atm) + 2R \ln x_w \end{aligned} \quad (24)$$

The value $\bar{h}_g - \bar{h}_w$ is obtained from Eqs. (22) and (24) by the thermodynamic identity $\bar{h}_w = \bar{\mu}_w + T\bar{s}_w$:

$$\begin{aligned} \bar{h}_g - \bar{h}_w = & \bar{h}_g - RA - \Phi_p + T\left(\frac{\partial\Phi_p}{\partial T}\right)_p - \bar{h}_{g,Haar}(T, 1atm) \\ & + \bar{h}_{g,Robie}(T, 1atm) - \sum_{i=1}^n w_{wi}x_i + \frac{1}{2} \sum_{i=1}^n \sum_{j=1}^n w_{ij}x_i x_j \end{aligned} \quad (25)$$

For phase transitions in pure, single-component systems, $\bar{h}_g - \bar{h}_w = T(\bar{s}_g - \bar{s}_w)$. Sahagian and Proussevitch use this relation in deriving $\bar{h}_g - \bar{h}_w$. Equations (24) and (25) cannot be reduced to give this relationship; but the values we calculate for $\bar{h}_g - \bar{h}_w$ of saturated albite using Eq. (25) are within 0.1% of $T(\bar{s}_g - \bar{s}_w)$, so we consider it appropriate here. The values of $\bar{s}_g - \bar{s}_w$ and $\bar{h}_g - \bar{h}_w$ are divided by the molecular weight of water to give $s_g - s_w$ and $h_g - h_w$ used in Eqs. (14) and (20).

Sahagian and Proussevitch (1996) use a somewhat different method, derived from Burnham and Davis (1974), to calculate $\bar{h}_g - \bar{h}_w$, for albite. A third method can be derived from relations given in Papale (1997) (see Appendix A). Zhang (1999) has also derived an expression for $h_g - h_w$ which takes into account the speciation of dissolved water into OH^- and molecular H_2O . We do not include Zhang's derivation because it depends on the value of an unknown constant.

The methods of Ghiorso and Sack (1995), Sahagian and Proussevitch (1996), and Papale (1997) all give values of $h_g - h_w$ on the order of hundreds of kilojoules per kilogram over pressures of tens to hundreds of megapascals (Fig. 2b). But the specific values of $h_g - h_w$

obtained by each method differ substantially at a given pressure, temperature, and composition. For example, albite values of $h_g - h_w$ from Sahagian and Proussevitch (1996) and Papale (1997) are higher than those from MELTS at $p < \sim 40$ MPa, and lower at $p > \sim 40$ MPa. MELTS values for rhyolite are lower at all pressures than those derived from Papale (1997). Above $p = \sim 130$ MPa, rhyolite values are negative using the values of MELTS, but not using values derived from Papale (1997). For albite, negative values are implied at $p > \sim 300$ MPa using calculations of Sahagian and Proussevitch, but not using values of MELTS or Papale (1997). Negative exsolution enthalpies at $p > \sim 400$ MPa are in fact implied by experiments of Holtz et al. (1995) for Qz–Ab–Or systems, and by experiments of Hamilton and Oxtoby (1986) for albite. The differences in values of $h_g - h_w$ reflect both the strengths and weaknesses in each formulation, and limitations of the data sets used to calibrate them. In the next section, we show that these differences do not significantly affect the temperature-change calculations.

Results

We solve equations Eqs. (14) and (20) using a fifth-order Cash–Karp Runge–Kutta solution (Press et al. 1992, pp. 713–715). We use the method of Ghiorso and Sack (1995) for calculating melt-related variables (v_m , $(\partial v_m/\partial T)$, c_{pm}) and equations from Haar et al. (1984) for gas properties [v_g , $(\partial v_g/\partial T)$, c_{pg}].

For comparison, we also calculate temperature changes for two cases that ignore the energetics of gas exsolution, using simplified equations for dT/dp at constant enthalpy:

$$\left(\frac{dT}{dp}\right)_h = \frac{-m_m[v_m - T(\frac{\partial v_m}{\partial T})] - m_g[v_g - T(\frac{\partial v_g}{\partial T})]}{m_g c_{pg} + m_m c_{pm}} \quad (26)$$

and constant entropy:

$$\left(\frac{dT}{dp}\right)_s = \frac{T\left\{m_m\left(\frac{\partial v_m}{\partial T}\right)_p + m_g\left(\frac{\partial v_g}{\partial T}\right)_p\right\}}{m_m c_{pm} + m_g c_{pg}} \quad (27)$$

In one case (denoted “case 1”), we let m_g and m_m vary as gas exsolves. In the second case (“case 2”), we hold m_g and m_m constant at the values they would have at $p = 0.1$ MPa. We maintain the same total amount of water (m_w) in each case. The case-2 solution is analogous to decompression of a fixed-ratio mixture of inert, compressible melt particles and gas (e.g., the conduit model of Buresti and Casarosa 1989).

Figure 3b shows the change in temperature of a water-saturated albite melt, initially at 900 °C, decompressing from $p = 200$ MPa to 0.1 MPa. This pressure range corresponds to ascent from about 8 km depth – comparable to the distance traveled by melt from Mount St. Helens on 18 May 1980 (e.g., Pallister et al. 1992).

The total water content of the system is assumed to remain constant at 7.75 wt% – equal to the saturation value of water in albite at 200 MPa.

For isenthalpic cooling, the full solution (upper solid line in Fig. 3b) gives lower temperatures than either solution that ignores the energetics of gas exsolution (the upper dashed and dotted lines). But the differences in final temperature amount to less than 25 °C. The full solution shows a slight increase in temperature with decreasing pressure from about 200–60 MPa, indicating that the heating effect of the shearing liquid dominates over the moderate cooling produced by isenthalpic decompression of the H₂O gas. At lower pressures, gas expansion and exsolution cause the bulk mixture to cool with decreasing pressure.

For the isentropic case, adiabatic cooling is substantial – roughly 200 ± 25 °C. Temperatures calculated by the full MELTS solution (lower solid line) lie between the case-1 and case-2 solutions that ignore the energy of gas exsolution. The latter two cases give final temperatures that are 31 °C below and 22 °C above the full MELTS solution, respectively, implying a difference in cooling of only about 12% from that given by the full solution. For comparison, Fig. 3b also shows isentropic decompression curves calculated using values of $s_g - s_w$ from Sahagian and Proussevitch (1996), and from relations derived from Papale (1997). The final temperature using the MELTS simulation does not differ by more

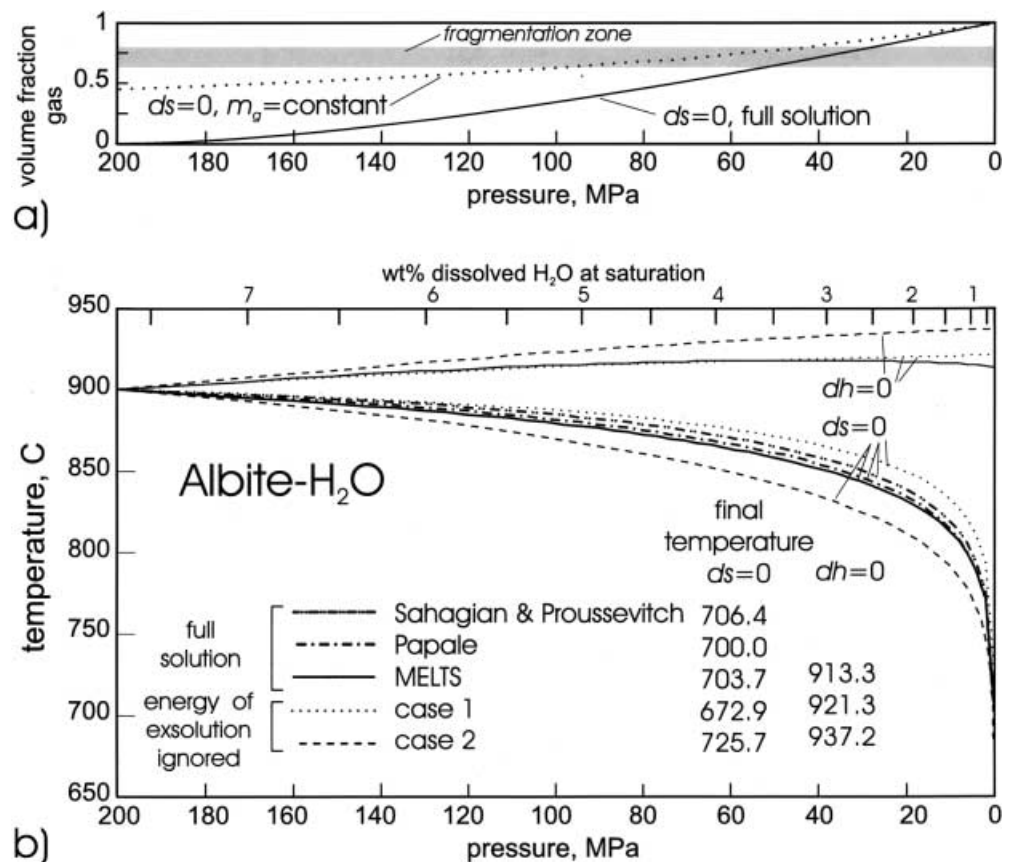
than a few degrees from that of Papale or Sahagian and Proussevitch. However, the latter two methods give lesser amounts of cooling at pressures > ~50 MPa than the MELTS formulation, as one would expect from the relative values of $h_g - h_w$ (and their implications regarding $s_g - s_w$) illustrated in Fig. 2b.

Using the MELTS formulation for exsolution enthalpy, we have repeated these calculations for water-saturated albite melts decompressing from $p_I \leq 200$ MPa, for T_I ranging from 700 to 1,100 °C. for $ds=0$, the full solution gives average cooling rates ranging from ~2.50 °C/MPa at $p_I < \sim 10$ MPa to ~0.75 °C/MPa for $p_I = 200$ MPa. For $p_I = 200$ MPa, T_f for solutions that ignore the energy of gas exsolution lie about 25 °C above (case 1) and below (case 2) T_f obtained from the full solution. For $dh=0$, both solutions that ignore gas exsolution tend to give final temperatures higher than the full solution, though all solutions are within about 150 °C of one another.

Effect on eruption velocities

The effect of gas exsolution on the velocity of erupting mixtures can be estimated by rearranging Eq. (1). If one ignores the gravitational term, one can calculate a maximum theoretical velocity of isentropically decompressing mixtures (u_{max}) by assuming that all the enth-

Fig. 3 a Volume fraction gas, and **b** pressure–temperature paths for a water-saturated albite–water mixture ($m_w = 0.0775$) decompressing from 200 MPa to 1 atm. In **a**, the total H₂O content of the mixture used in the full solution (solid line) and the case-2 solution (dotted line) are the same, but in the case-2 solution, nearly all of the H₂O resides in the gas phase throughout decompression, producing the high total volume-fraction gas plotted here



alpy change is converted to kinetic energy:

$$u_{\max} = \sqrt{2(h_1 - h_f)} \quad (28)$$

This method was used by Mastin (1995b) for non-juvenile eruptions, and by Wilson (1980) for Plinian eruptions to calculate maximum theoretical velocities as a function of initial pressure. The two studies ignored the energy associated with gas exsolution and assumed that the mass fraction gas did not change with pressure. In these respects, their analysis was the same as the case-2 approach that ignores gas exsolution. Wilson (1980) (but not Mastin 1995b) made the additional assumption that the gas obeyed the ideal gas relation.

As shown in Fig. 4a, the solutions that take gas exsolution into account (solid lines) give u_{\max} of a few to several hundred meters per second for initial pressures of 10 MPa or more. Case-2 solutions that ignore gas exsolution give u_{\max} values that are several percent higher (amounting to a few to several tens of meters per second). The higher u_{\max} values of these case-2 solutions result from the existence of a gas phase throughout decompression that can expand, and from the fact that no energy is expended in gas exsolution.

Figure 4b gives the total enthalpy released as these mixtures decompress isentropically to 1 atm pressure. The energy released is roughly an order of magnitude less than that released by explosives (2–2.2 MJ/kg for gunpowder; ~ 4.5 MJ/kg for TNT) and somewhat less than the maximum available from decompressed melt–water mixtures (~ 0.4 – 0.45 MJ/kg; Wohletz 1986; Mastin 1995b). If the assumptions of Eq. (1) are correct, this energy must go into lifting and acceleration. If the assumptions are false, some fraction may be used to heat, deform, or accelerate the surroundings. The generation of seismic waves, shock waves, and crushing or ejection of wall rock may all be driven by this energy.

Using Fig. 4b as a reference, it is important to note the following:

1. Energy of lifting is a significant fraction of Δh . The energy of lifting is about 10 J/kg per meter of magma ascent. If we assume that these mixtures originate at pressures that are roughly lithostatic for their depth, the energy required for lifting (shaded area in Fig. 4b) is about 25–45% of the total isentropic enthalpy loss.
2. Below the fragmentation depth, kinetic energy is negligible. Conduit models (Wilson et al. 1980; Papale and Dobran 1993; Mastin 1995b; Papale et al. 1998) calculate ascent velocities of tens of meters per second or less at depths below that where magma fragments into a gas–ash mixture. The kinetic energy of these mixtures (< 1 kJ/kg) is insignificant relative to the isentropic enthalpy loss and small compared to lifting energy for mixtures that rise hundreds or thousands of meters.
3. Above the fragmentation depth, efficiency of energy conversion is controlled largely by conduit geometry. In conduits that do not flare outward immediately below the surface, the mixture velocity cannot exceed

its sonic velocity. If the conduit flares, but not sufficiently to allow the mixture to decompress to atmospheric pressure at the exit, the final velocity will be supersonic but less than its maximum theoretical velocity. If the vent flares more than required to reach atmospheric pressure, normal shocks will develop in the vent that drop the exit velocity to subsonic values. These factors tend to constrain exit velocities to sonic values of roughly 70–150 m/s (Fig. 4a), which are a fraction of their maximum theoretical values. Corresponding kinetic energies (< 10 kJ/kg) are also a small fraction of that available during isentropic enthalpy loss.

Effect on viscosity

Changes in temperature affect the melt viscosity, which in turn may affect all other flow properties. Figure 5 illustrates the change in viscosity with pressure of water-saturated basalt ($T_f = 1150$ °C) and rhyolite ($T_f = 750$ °C), respectively, decompressing from $p = 200$ to 0.1 MPa. For basalt, isentropic cooling increases viscosity by nearly a factor of 15 over its initial value. But the thermal effect of gas exsolution increases viscosity only about 10% more than the case-2 method that ignores the energy of exsolution. For rhyolite, the removal of water from the melt during decompression causes an extreme increase in viscosity (from 6×10^6 Pa s at $p = 200$ MPa to 1.5×10^{12} Pa s at $p = 1$ atm) even under constant-temperature conditions. Isentropic cooling increases the melt viscosity by an additional 2.5 orders of magnitude. Isenthalpic heating decreases melt viscosity by about 0.7 orders of magnitude relative to that at $T = 750$ °C. But in both the isentropic and isenthalpic cases, solutions that consider gas exsolution produce final viscosities that differ by less than 20% from those that ignore energy of gas exsolution.

Adiabatic, isentropic cooling is most important when the melt–gas mixture is fragmenting and approaching its maximum velocity at the top of the conduit. As noted by Dingwell and Webb (1989), melt will fail brittlely when the extensional strain exceeds a value ($\dot{\epsilon}_{crit}$) that can be accommodated by viscous deformation. Following Maxwell's relation,

$$\dot{\epsilon}_{crit} = K \frac{G_{\infty}}{\eta_m} \quad (29)$$

where G_{∞} is the elastic shear modulus of the material (equal to about 20 GPa) and K is an empirical constant (equal to ~ 0.01 ; Dingwell and Webb 1989). Extensional strain within the conduit is probably responsible for fragmentation of the erupting mixture (Papale 1999). The beginning of fragmentation may be slightly delayed by isenthalpic heating below the fragmentation depth. But once fragmentation begins, acceleration becomes significant and adiabatic cooling may enhance the fragmentation process. A 10- to 100-fold increase in viscosity due to adiabatic cooling at the top of the

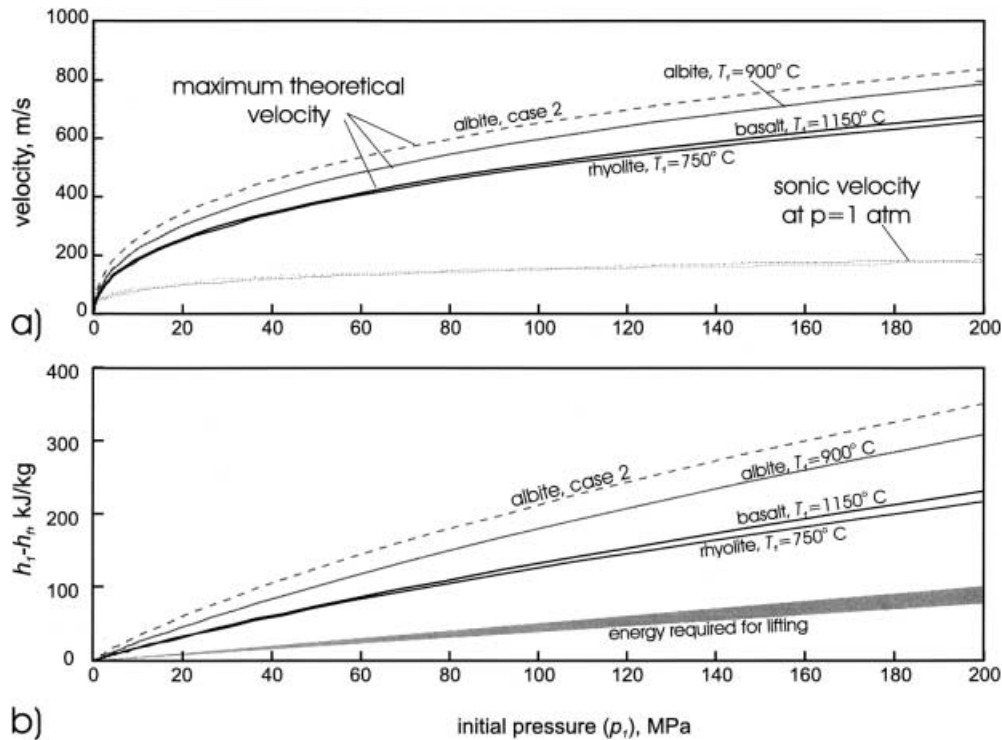


Fig. 4 **a** Maximum theoretical velocity versus initial pressure for isentropically decompressed mixtures of water-saturated albite, basalt, and rhyolite. Compositions of these melts are given in Table 2. *Solid lines* give u_{max} calculated using the full solution for gas exsolution. *Dashed line* represents u_{max} for albite ($T_i = 900^\circ\text{C}$) using the case-2 solution that ignores the energy of gas exsolution. For reference, *dotted lines* give the sonic velocities of these mixtures at 1 atm pressure, calculated using methods explained in Appendix D. **b** Enthalpy loss of the melt–gas mixture described in **a** during isentropic decompression to 1 atm. As in **a**, *solid lines* give enthalpy loss using the full solution that considers the energy of gas exsolution; *dashed line* gives the enthalpy loss for water-saturated albite using the case-2 solution that ignores gas exsolution. The *shaded area* gives the energy required ($g\Delta z$) to lift this magma from its initial position in the Earth’s crust to the surface, assuming that its initial pressure corresponds to lithostatic pressure at a given depth and that the lithostatic pressure gradient is 20–25 MPa/km

Table 2 Compositions of melts used in this paper. Oxide compositions are wt% of an anhydrous melt. Basalt is a MORB composition taken from Table 2 of Dixon et al. (1995). Rhyolite composition represents a haplogranitic melt (HPG8) characterized for its solubility (Holtz et al. 1995) and rheologic properties (e.g., Dingwell et al. 1996; Hess and Dingwell 1996)

Property	Basalt	Albite	Rhyolite
Temperature ($^\circ\text{C}$)	1,150	900	750
SiO ₂	50.8	68.74	76.69
Al ₂ O ₃	13.7	19.44	12.91
Fe ₂ O ₃	0	0	61
FeO	12.4	0	55
MgO	6.67	0	04
CaO	11.5	0	29
TiO ₂	1.84	0	1
Na ₂ O	0.68	11.82	4.2
K ₂ O	0.15	0	4.61

conduit should reduce the critical strain rate by a similar amount, causing the melt to break up more thoroughly than might be the case under isothermal conditions.

Summary and discussion

Our main findings are as follows:

- Adiabatic cooling in erupting mixtures can be significant in cases where there is little friction to impede flow. But 85–90% of this cooling results from expansion of gas that exists in the system rather than the thermal effects of gas exsolution.
- The relatively small effect of gas exsolution energy on cooling is independent of which model (Sahagian and Proussevitch; Papale, or Ghiorso and Sack) is used to calculate exsolution energy.
- Two main factors act to limit the efficiency of erupting mixtures in converting enthalpy to kinetic energy: below the fragmentation depth, the limiting factor is viscous resistance to flow; above the fragmentation depth, the limiting factor is conduit geometry.

This analysis considers only the effects of gas exsolution and expansion on temperature changes. The heat of crystallization is on the order of several hundred kilojoules per kilogram (Berman 1988; Ghiorso and Sack 1995), which is similar in magnitude but opposite in sign to the heat of gas exsolution ($h_g - h_w$). Thus crystallization of a few weight percent minerals could increase temperatures by several degrees Celsius, effectively negating the cooling effect of gas exsolution. Crystallization during ascent in conduits has been

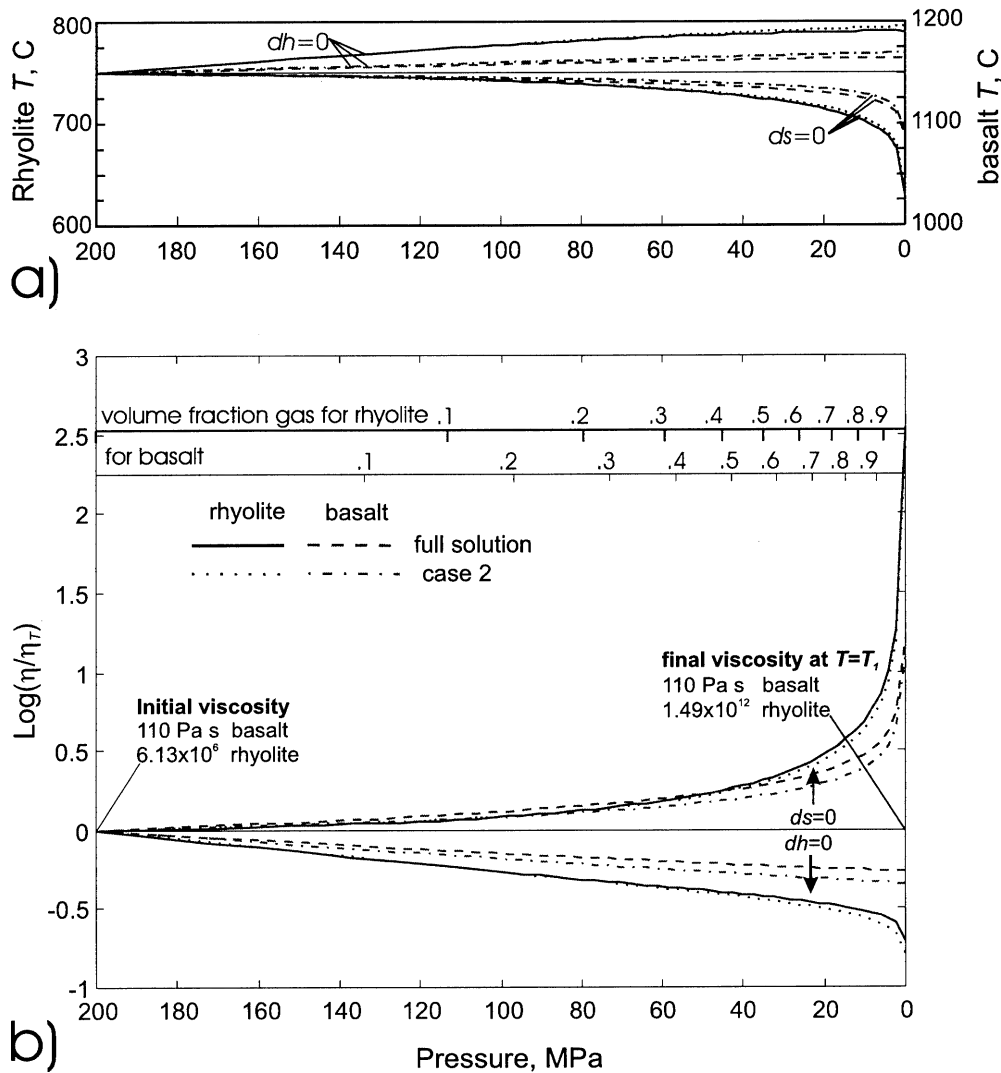


Fig. 5 **a** Temperature of decompressing melt–gas mixtures of (1) water-saturated basalt, initially at $T=1,150$ °C ($m_w=0.0418$), and (2) water-saturated rhyolite, initially at $T=750$ °C ($m_w=0.0534$), during decompression from $p_i=200$ MPa to $p_f=1$ atm. The *solid lines* represent the full solution for rhyolite under isenthalpic (*upper line*) and isentropic (*lower line*) conditions. The *upper and lower dotted lines* represent $dh=0$ and $ds=0$ solutions, respectively, for rhyolite under case-2 conditions that ignore the energy of gas exsolution. *Upper and lower dashed lines* represent the full $dh=0$ and $ds=0$ solutions, respectively, for basalt. *Upper and lower dash-dotted lines* represent the $dh=0$ and $ds=0$ solutions, respectively, for case-2 decompression of basalt. The mixtures contain no exsolved gas at the initial pressure. Compositions of the melts are given in Table 2. **b** Log of the viscosity (η) of a decompressing melt at the temperature given in **a**, normalized to the viscosity of the same melt (η_T) at $T=T_i$, as a function of pressure. The line patterns in **b** denote the same conditions for decompression as those in **a**. Viscosities are calculated using relations in Ryan and Blevins (1987) for basalt, and Hess and Dingwell (1996) for rhyolite inferred for sub-Plinian andesitic eruptions (e.g., Gardner et al. 1998).

Perhaps the greatest thermal effect on eruption processes is not the average temperature change but the concentration of temperature changes in certain parts of the system. In the shallow vent area, for example, highly

transient pressure drops of a few megapascals may cool the gas phase by a few hundred degrees before it can equilibrate with solid particles. The temperature difference between gas and melt could freeze the rims of expanding pyroclasts and promote their disintegration. In deep conduits, if all of the heat generated by isenthalpic decompression were concentrated along conduit margins where shearing is greatest, the viscosity in those marginal areas could decrease by multiple orders of magnitude, dramatically reducing flow resistance. For example, using the isenthalpic rhyolite decompression scenario illustrated in Fig. 5 and concentrating all the generated heat into 20% of the magma–gas mixture, that portion of the mixture would heat up to about 200 °C and its viscosity would decrease by about 4.5 orders of magnitude.

Fujii and Uyeda (1974) argued that instability of this nature (termed “thermal runaway”) may account for unstable alternations between explosive and effusive volcanism. Hardee and Larson (1977) found that viscous shearing could dramatically increase melt viscosity even in small (<1 m wide), rapidly emplaced dikes and

conduits in which conductive heat loss to the host rock was significant. Recent papers have suggested volatile-dependent viscosity (Wylie et al. 1999) and stick-slip conditions along the wall of a conduit (Denlinger and Hoblitt 1999) to explain cycles of effusion and explosions, apparently without consideration of thermal effects. The process of thermal instability may be highly significant and merits further study.

Acknowledgements This paper has benefitted from careful reviews by Margaret Mangan, Jacob Lowenstern, and Joseph Walder of the US Geological Survey; by Ken Wohletz of Los Alamos National Laboratory; and by Donald Dingwell of the Universität München.

Appendix A: Values of $\bar{s}_g - \bar{s}_w$ derived from Papale (1997)

Papale (1997) presents a thermodynamic model that predicts solubility of CO₂ or H₂O in silicate melts as a function of composition, temperature, and pressure. His model provides the most accurate prediction available for water solubility in melts of any composition, and therefore his thermodynamic relations, including $\bar{s}_g - \bar{s}_w$, may be more accurate than other models.

Papale gives the following expression for the activity coefficient (γ_w) of dissolved water in a melt

$$RT \ln \gamma_w = (1 - x_w) \sum_{i=1}^n x_i w_{wi} - \sum_{i=1}^{n-1} \sum_{j=i+1, j \neq w}^n x_i x_j w_{ij} \quad (\text{A1})$$

The terms w_{ij} are interaction coefficients, taken from Ghiorso et al. (1983), and the terms x_i , x_j are mole fractions of anhydrous oxides, defined in Ghiorso et al. (1983). For the interaction coefficients involving water (w_{wi}), Papale derives his own values.

The fugacity of dissolved water in its standard state, f_w^o , is given by Papale as:

$$\ln f_w^o = \ln f_w^o(p^o, T^o) + \int_{p^o}^p \frac{\bar{v}_w}{RT} dp - \int_{T^o}^T \frac{1}{RT^2} \int_{p^o}^p \left[\bar{v}_w - T \left(\frac{\partial \bar{v}_w}{\partial T} \right)_p \right] dpdT \quad (\text{A2})$$

where p^o and T^o are the standard-state pressure and temperature, 0 Pa and 1,000 K; and \bar{v}_w is the partial molar volume of dissolved water. Papale gives an empirically derived value for $\ln f_w^o(p^o, T^o)$ (19.3347), and uses a 3-D polynomial expression for \bar{v}_w , as a function of p and T , derived from Burnham and Davis (1974), which can be integrated or differentiated to evaluate the expressions above.

The chemical potential of dissolved water in the melt ($\bar{\mu}_w$) is defined as:

$$\bar{\mu}_w = \bar{\mu}_w^o + RT \ln \frac{f_w}{f_w^o} \quad (\text{A3a})$$

$$= \bar{\mu}_w^o + RT \ln \gamma_w x_w \quad (\text{A3b})$$

where $\bar{\mu}_w^o$ is the standard-state chemical potential of water in the melt (i.e., the molar Gibbs free energy of “pure” dissolved water at p and T). At saturation, $\bar{\mu}_g = \bar{\mu}_w$ and $f_g = f_w \approx p$ (the approximation is made by Papale). Thus (A3a) can be rearranged to find $\bar{\mu}_w^o$:

$$\bar{\mu}_w^o = \bar{\mu}_g - RT \ln \frac{p}{f_w^o} = \bar{\mu}_g - RT \ln p + RT \ln f_w^o(p^o, T^o) + \int_{p^o}^p \bar{v}_w dp - \int_{T^o}^T \frac{1}{T} \int_{p^o}^p \left[\bar{v}_w - T \left(\frac{\partial \bar{v}_w}{\partial T} \right)_p \right] dpdT \quad (\text{A4})$$

Substituting (A4) and (A1) into (A3b), the chemical potential of dissolved water can be derived:

$$\bar{\mu}_w = \bar{\mu}_g - RT \ln p + RT \ln f_w^o(p^o, T^o) + \int_{p^o}^p \bar{v}_w dp - \int_{T^o}^T \frac{1}{T} \int_{p^o}^p \left[\bar{v}_w - T \left(\frac{\partial \bar{v}_w}{\partial T} \right)_p \right] dpdT + (1 - x_w) \sum_{i=1}^n x_i w_{wi} - \sum_{i=1}^{n-1} \sum_{j=i+1, j \neq w}^n x_i x_j w_{ij} + RT \ln x_w \quad (\text{A5})$$

Taking $-(\partial \bar{\mu}_w / \partial T)$, we derive the entropy:

$$\bar{s}_w = \bar{s}_g + R \ln p - R \ln f_w^o(p^o, T^o) - \frac{\partial}{\partial T} \left(\int_{p^o}^p \bar{v}_w dp \right) + \frac{\partial}{\partial T} \left\{ \int_{T^o}^T \frac{1}{T} \int_{p^o}^p \left[\bar{v}_w - T \left(\frac{\partial \bar{v}_w}{\partial T} \right)_p \right] dpdT \right\} - R \ln x_w \quad (\text{A6})$$

The difference $\bar{s}_g - \bar{s}_w$ can be derived as:

$$\bar{s}_g - \bar{s}_w = -R \ln p + R \ln f_w^{oL}(p^o, T^o) + \frac{\partial}{\partial T} \left(\int_{p^o}^p \bar{v}_w dp \right) - \frac{\partial}{\partial T} \left\{ \int_{T^o}^T \frac{1}{T} \int_{p^o}^p \left[\bar{v}_w - T \left(\frac{\partial \bar{v}_w}{\partial T} \right)_p \right] dpdT \right\} + R \ln x_w \quad (\text{A7})$$

Each of these terms is converted to per-kilogram values by dividing them by the molecular weight of water. For pressures of 10⁻¹–10² MPa, the order of magnitude values of the terms on the right side of Eq. (A7) are 10², 10², 10⁰, 10⁻², and 10¹ J/mol K, respectively, suggesting that the first two terms dominate.

Papale (1997) also uses a formulation for solubility of CO₂. Using a derivation similar to that above, the equation of entropy for dissolved CO₂ has same form as shown in Eq. (A7) for water. For CO₂, each of the terms in Eq. (A7) should have roughly the same order of magnitude values as those for water. Therefore we would expect the exsolution enthalpy, and entropy, for CO₂ to be of the same order of magnitude as that for water.

Appendix B: Calculating dm_m

We begin this derivation by pointing out that the change in m_m is due entirely to removal of dissolved water in the melt – the mass of all other components remains constant. The mass fraction of dissolved water in the melt is \hat{m}_w , defined as:

$$\hat{m}_w = \frac{\hat{M}_w}{\sum_{i=1}^n \hat{M}_i + \hat{M}_w} \quad (\text{B1})$$

where \hat{M}_w is the total mass of dissolved water (in kg) in a given mass of melt, and \hat{M}_i are the masses of all other components in the melt. The denominator on the right-hand side of the equation is the total mass of the melt, \hat{M}_{tot} , in kilograms. Differentiating this equation, and holding the mass of all anhydrous components constant, we get:

$$d\hat{m}_w = \left[\frac{1}{\hat{M}_{tot}} - \frac{\hat{M}_w}{\hat{M}_{tot}^2} \right] d\hat{M}_w = \frac{(1 - \hat{m}_w)}{\hat{M}_{tot}} d\hat{M}_w \quad (\text{B2})$$

The term \hat{m}_w can also be differentiated from Eq. (B3) as follows:

$$d\hat{m}_w = \sigma \beta p^{\beta-1} dp = \hat{m}_w \frac{\beta}{p} dp \quad (\text{B3})$$

which can be substituted into Eq. (B2) and rearranged to give:

$$d\hat{M}_w = \frac{\hat{M}_{tot} \hat{m}_w}{(1 - \hat{m}_w)} \frac{\beta}{p} dp \quad (\text{B4})$$

Dividing both sides by M_{tot} and substituting m_m for \hat{M}_{tot}/M_{tot} (the mass of the melt divided by the mass of the melt + gas system), we get:

$$dm_m = \frac{m_m \hat{m}_w}{(1 - \hat{m}_w)} \frac{\beta}{p} dp \quad (\text{B5})$$

Appendix C: Calculating $(\partial h_m / \partial \hat{M}_w) d\hat{M}_w$ and $(\partial s_m / \partial \hat{M}_w) d\hat{M}_w$

Following regular solution theory (Ghiorso et al. 1983), the molar enthalpy of a melt is the sum of the partial molar enthalpies of its components, multiplied by the mole fraction of each component:

$$\bar{h}_m = \sum_{i=1}^n x_i \bar{h}_i \quad (\text{C1})$$

The partial molar enthalpy of each component is a function of both the enthalpy per mole of that component (e.g., SiO₂, TiO₂) in its pure form and at a given p and T , and the enthalpy of mixing. Similarly, the molar entropy of a melt, \bar{s}_m , is a weighted sum of its partial molar components. For convenience, we define the

specific (per-kilogram) enthalpy and entropy of a melt by a similar formula:

$$h_m = \sum_{i=1}^n \hat{m}_i h_i = \sum_{i=1}^n \left(\frac{\hat{M}_i h_i}{\sum_{j=1}^n \hat{M}_j} \right) \quad (\text{C2})$$

$$s_m = \sum_{i=1}^n \hat{m}_i s_i = \sum_{i=1}^n \left(\frac{\hat{M}_i s_i}{\sum_{j=1}^n \hat{M}_j} \right) \quad (\text{C3})$$

where \hat{m}_i is the mass fraction of that component in the melt. The denominator within the parentheses is the total mass of the melt, \hat{M}_{tot} .

Differentiating Eqs. (C2) and (C3) with respect to \hat{M}_w while holding the mass of other components constant, we obtain:

$$\frac{\partial h_m}{\partial \hat{M}_w} = \frac{1}{\hat{M}_{tot}} (h_w - h_m) \quad (\text{C4})$$

$$\frac{\partial s_m}{\partial \hat{M}_w} = \frac{1}{\hat{M}_{tot}} (s_w - s_m) \quad (\text{C5})$$

where h_w and s_w are the partial specific enthalpy and entropy of dissolved water, respectively. We then multiply these terms by the expression for $d\hat{M}_w$ [Eq. (B4)] to give:

$$\left(\frac{\partial h_m}{\partial \hat{M}_w} \right) d\hat{M}_w = \frac{\hat{m}_w}{(1 - \hat{m}_w)} \frac{\beta}{p} (h_w - h_m) dp \quad (\text{C6})$$

$$\left(\frac{\partial s_m}{\partial \hat{M}_w} \right) d\hat{M}_w = \frac{\hat{m}_w}{(1 - \hat{m}_w)} \frac{\beta}{p} (s_w - s_m) dp \quad (\text{C7})$$

Appendix D: Calculation of sonic velocities

Sonic velocities of melt–gas mixtures in Fig. 4a were calculated from the relation:

$$C = \sqrt{\frac{k_s}{\rho}} \quad (\text{D1})$$

where C is sonic velocity (m/s), k_s is the bulk modulus of the melt–gas mixture at constant entropy, and ρ is the mixture density. [The isentropic bulk modulus, k_s , is related to the more commonly used isothermal bulk modulus, k_T , by the relation $k_s = (c_v/c_p)k_T$]. The isentropic bulk modulus of the mixture is calculated as:

$$\frac{1}{k_s} = \frac{\phi}{k_g} + \frac{1 - \phi}{k_m} \quad (\text{D2})$$

where k_g and k_m are the isentropic bulk moduli of the gas and melt, respectively, which are defined as $k \equiv \rho(\partial p / \partial \rho)_s$ (the subscript s indicates constant entropy). At 1 atm, k_g for an ideal gas is simply equal to (c_{pg}/c_{vg}) times the pressure in Pascals, or $[1.23 \times (1.013 \times 10^5 \text{ Pa}) = 1.25 \times 10^5 \text{ Pa}$ for H₂O gas at $T = 900 \text{ }^\circ\text{C}$]. We use values of k_m ranging from 1.2 to $1.6 \times 10^{11} \text{ Pa}$, obtained from

calculations of density and its derivative with respect to pressure calculated from MELTS. The ϕ is the volume fraction gas in the mixture, which is calculated from the mass fractions exsolved gas and melt in the mixture and their densities. At 1 atm pressure, ϕ is generally above 0.99, meaning that the right-hand term on the right side of Eq. (D2) is generally insignificant.

The density of the mixture is calculated as:

$$\frac{1}{\rho} = \frac{m_g}{\rho_g} + \frac{m_m}{\rho_m} \quad (\text{D3})$$

where the densities of the gas and melt are calculated using relations in Haar et al. (1984) and Ghiorso and Sack (1995), respectively.

References

- Berman RG (1988) Internally consistent thermodynamic data for minerals in the system $\text{Na}_2\text{O}-\text{K}_2\text{O}-\text{CaO}-\text{MgO}-\text{FeO}-\text{Fe}_2\text{O}_3-\text{Al}_2\text{O}_3-\text{SiO}_2-\text{TiO}_2-\text{H}_2\text{O}-\text{CO}_2$. *J Petrol* 29:445–522
- Buresti G, Casarosa C (1989) One-dimensional adiabatic flow of equilibrium gas-particle mixtures in long vertical ducts with friction. *J Fluid Mech* 203:251–272
- Burnham CW, Davis NF (1971) The role of H_2O in silicate melts. I. P–V–T relations in the system $\text{NaAlSi}_3\text{O}_8-\text{H}_2\text{O}$ to 10 kilobars and 1000 °C. *Am J Sci* 270:54–79
- Burnham CW, Davis NF (1974) The role of H_2O in silicate melts: II. Thermodynamic and phase relations in the system $\text{NaAl}_3\text{SiO}_8-\text{H}_2\text{O}$ to 10 kilobars, 700 to 1100 °C. *Am J. Sci* 274:902–940
- Denlinger RP, Hoblitt RP (1999) Cyclic eruptive behavior of silicic volcanoes. *Geology* 27:459–462
- Dingwell DB, Webb SL (1989) Structural relaxation in silicate melts and non-Newtonian melt rheology in geologic processes. *Phys Chem Miner* 16:508–516
- Dingwell DB, Romano C, Hess K-U (1996) The effect of water on the viscosity of a haplogranitic melt under P–T–X conditions relevant to silicic volcanism. *Contrib Mineral Petrol* 124:19–28
- Dixon JE, Stolper EM, Holloway JR (1995) An experimental study of H_2O and carbon dioxide solubilities in mid-ocean ridge basaltic liquids. Part I: Calibration and solubility results. *J Petrol* 36:1607–1631
- Dobran F (1992) Nonequilibrium flow in volcanic conduits and application to the eruptions of Mt. St. Helens on May 18, 1980 and Vesuvius in AD 79. *J Volcanol Geotherm Res* 49:285–311
- Eichelberger JC, Carrigan CR, Westrich HR, Price RH (1986) Non-explosive silicic volcanism. *Nature* 323:598–602
- Fujii N, Uyeda S (1974) Thermal instabilities during flow of magma in volcanic conduits. *J Geophys Res* 79:3367–3369
- Gardner CA, Cashman KV, Neal CA (1998) Tephra-fall deposits from the 1992 eruption of Crater Peak, Alaska: implications of clast textures for eruptive processes. *Bull Volcanol* 59:537–555
- Ghiorso MS, Sack RO (1995) Chemical mass transfer in magmatic processes. IV: A revised and internally consistent thermodynamic model for the interpolation and extrapolation of liquid–solid equilibria in magmatic systems at elevated temperatures and pressures. *Contrib Mineral Petrol* 119:197–212
- Ghiorso MS, Carmichael ISE, Rivers ML, Sack RO (1983) The Gibbs free energy of mixing of natural silicate liquids; an expanded regular solution approximation for the calculation of magmatic intensive variables. *Contrib Mineral Petrol* 84:107–145
- Gibert G, Wilson L (1990) The influence of geometry on the ascent of magma in open fissures. *Bull Volcanol* 52:515–521
- Haar L, Gallagher JS, Kell GS (1984) NBS/NRC steam tables. Hemisphere Publ Corp, New York
- Hamilton DL, Oxtoby S (1986) Solubility of water in albite-melt determined by the weight-loss method. *J Geol* 94:626–630
- Hardee HC, Larson DW (1977) Viscous dissipation effects in magma conduits. *J Volcanol Geotherm Res* 2:299–308
- Hayba DO, Ingebritsen SE (1997) Multiphase groundwater flow near cooling plutons. *J Geophys Res* 102:12235–12252
- Hess K-U, Dingwell DB (1996) Viscosities of hydrous leucogranitic melts: a non-Arrhenian model. *Am Mineral* 81:1297–1300
- Holtz F, Behrens H, Dingwell DB, Johannes W (1995) H_2O solubility in haplogranitic melts: compositional, pressure, and temperature dependence. *Am Mineral* 80:94–108
- Jaupart C, Allègre CJ (1991) Gas content, eruption rate and instabilities of eruption regime in silicic volcanoes. *Earth Planet Sci Lett* 102:413–429
- Kieffer SW (1981) Fluid dynamics of the May 18 blast at Mount St. Helens. In: Lipman, PW, Mullineaux DR (eds) *The 1980 eruptions of Mount St. Helens*, Washington. US Geol Surv Prof Pap 1250, pp 379–400
- Kieffer SW (1984) Factors governing the structure of volcanic jets. In: National Research Council (eds) *Explosive volcanism, inception, evolution, and hazards*. National Academy Press, Washington, DC, pp 143–157
- Kieffer SW, Delany JM (1979) Isentropic decompression of fluids from crustal and mantle pressures. *J Geophys Res* 84:1611–1620
- Liepmann HW, Roshko A (1957) *Elements of gasdynamics*. Wiley, New York
- Mastin LG (1995a) A numerical program for steady-state flow of Hawaiian magma–gas mixtures through vertical eruptive conduits. US Geol Surv Open-File Rep 95–756
- Mastin LG (1995b) Thermodynamics of gas and steam-blast eruptions. *Bull Volcanol* 57:85–98
- Mastin LG (1997) Evidence for water influx from a caldera lake during the explosive hydromagmatic eruption of 1790, Kilauea Volcano, Hawaii. *J Geophys Res* 102:20093–20109
- Mastin, LG (2000) A numerical program for steady-state flow of magma–gas mixtures through vertical eruptive conduits. US Geol Surv Open-File Rep 00-209 (available at <http://vulcan.wr.usgs.gov/Projects/Mastin/OFR00209.pdf>)
- Moran MJ, Shapiro HN (1992) *Fundamentals of engineering thermodynamics*. Wiley, New York
- Muffer LJP, White DE, Truesdell AH (1971) Hydrothermal explosion craters in Yellowstone National Park. *Geol Soc Am Bull* 82:723–740
- Nicholls J (1980) A simple model for estimating the solubility of H_2O in magmas. *Contrib Mineral Petrol* 74:211–220
- Nicholls J, Stout MZ (1982) Heat effects of assimilation, crystallization, and vesiculation in magmas. *Contrib Mineral Petrol* 81:328–339
- Ochs FA, Lange RA (1997) The partial molar volume, thermal expansivity and compressibility of dissolved H_2O in $\text{NaAlSi}_3\text{O}_8$ liquid: new measurements and an internally consistent model. *Contrib Mineral Petrol* 129:155–165
- Ochs FA, Lange RA (1999) The density of hydrous magmatic liquids. *Science* 283:1314–1317
- Pallister JS, Hoblitt RP, Crandell DR, Mullineaux DR (1992) Mount St. Helens a decade after the 1980 eruptions: magmatic models, chemical cycles, and a revised hazards assessment. *Bull Volcanol* 54:126–146
- Papale P (1997) Modeling of the solubility of a one-component H_2O or CO_2 fluid in silicate melts. *Contrib Mineral Petrol* 126:237–251
- Papale P (1999) Strain-induced magma fragmentation in explosive eruptions. *Nature* 397:425–428
- Papale P, Dobran F (1993) Modeling the ascent of magma during the Plinian eruption of Vesuvius in A.D. 79. *J Volcanol Geotherm Res* 58:101–132
- Papale P, Neri A, Macedonio G (1998) The role of magma composition and water content in explosive eruptions I. Conduit dynamics. *J Volcanol Geotherm Res* 87:75–93
- Press WH, Teukolsky SA, Vetterling WT, Flannery BP (1992) *Numerical recipes in Fortran 77*, 2nd edn. Cambridge University Press, Cambridge

- Proussevitch AA, Sahagian DL (1998) Dynamics and energetics of bubble growth in magmas; analytical formulation and numerical modeling. *J Geophys Res* 103(8):18223–18251
- Robie RA, Hemingway BS, Fisher JR (1978) Thermodynamic properties of minerals and related substances at 298.15 K and 1 bar (10^5 Pascals) pressure and at higher temperature. *US Geol Surv Bull* 1452
- Ryan MP, Blevins JYK (1987) The viscosity of synthetic and natural silicate melts and glasses at high temperatures and 1 bar (10^5 Pascals) pressure and at higher pressures. *US Geol Surv Bull* 1764
- Saad MA (1985) *Compressible fluid flow*. Prentice-Hall, Englewood Cliffs
- Sahagian DL, Proussevitch AA (1996) Thermal effects of magma degassing. *J Volcanol Geotherm Res* 74:19–38
- Silver L, Stolper E (1985) A thermodynamic model for hydrous silicate melts. *J Geol* 93:161–178
- White DE (1955) Violent mud-volcano eruptions of Lake City Hot Springs, northeastern California. *Geol Soc Am Bull* 66:1109–1130
- Wilson L (1980) Relationships between pressure, volatile content and ejecta velocity in three types of volcanic explosion. *J Volcanol Geotherm Res* 8:297–313
- Wilson L, Sparks RSJ, Walker GPL (1980) Explosive volcanic eruptions–IV. The control of magma properties and conduit geometry on eruption column behaviour. *Geophys J R Astron Soc* 63:117–148
- Wohletz KH (1986) Explosive magma–water interactions: thermodynamics, explosion mechanisms, and field studies. *Bull Volcanol* 48:245–264
- Wohletz KH, Valentine GA (1990) Computer simulations of volcanic eruptions. In: Ryan MP (ed) *Magma transport and storage*. Wiley, New York, pp 113–135
- Woods A (1995) The dynamics of explosive volcanic eruptions. *Rev Geophys* 33:495–530
- Wylie J, Voight B, Whitehead JA (1999) Instability of magma flow from volatile-dependent viscosity. *Science* 285:1883–1885
- Zhang Y (1999) Exsolution enthalpy of water from silicate liquids. *J Volcanol Geotherm Res* 88:201–207